Effect of NAPL entrapment conditions on air sparging remediation efficiency

W.A.P. Waduge [a], K. Soga [a,*], J. Kawabata [b]

[a] *Engineering Department, University of Cambridge, Cambridge, UK*
[b] *Kajima Technical Research Institute, Tokyo, Japan*

Abstract

The effect of soil heterogeneity and the entrapment condition of NAPL source on the mass removal efficiency of air sparging coupled with soil vapour extraction (AS/SVE) was investigated using an intermediate scale two-dimensional laboratory soil tank. Four different NAPL entrapments were created by varying the height of the water table in heterogeneous soil models. Different mass removal efficiencies were achieved for different NAPL entrapment conditions, which were governed by soil heterogeneity and water table height before and during AS/SVE operation. Remobilization and redistribution of toluene and water improved the mass removal. Overall results suggested that it was difficult to achieve the complete remediation of NAPL source due to complex entrapment in heterogeneous soil system. In order to assess the potential contamination in the post-remediation stage, gas and dissolved concentrations of toluene were measured after the AS/SVE operation. The results showed that gas concentration close to remaining NAPL source zone increased rapidly and reached to steady state values, which were much smaller than the vapour pressure, whereas the aqueous phase concentrations increased continuously toward the solubility limit.
© 2004 Elsevier B.V. All rights reserved.

Keywords: Air sparging; Source zone; Remediation; Mass transfer; Laboratory investigation

1. Introduction

Air sparging is one of the popular techniques, which are used in remediation of subsurface contaminated with volatile organic compounds (VOCs) and chlorinated solvents [1]. In air sparging operation, air is injected into or below contaminated aquifer. The injected air rises through saturated zone towards unsaturated zone due to buoyancy effect. As the air passes through either non-aqueous phase liquids (NAPLs) or contaminated groundwater, VOCs are stripped into air channels where they are carried into the unsaturated zone. Once the contaminated air comes to the unsaturated zone, it is extracted using soil vapour extraction system. By applying vacuum into the subsurface and hence inducing a pressure gradient towards the extraction well, soil vapour extraction system controls the air movement in the subsurface, preventing migration of the contaminated air into uncontaminated areas. Injection of air into the subsurface also increases the dissolved oxygen concentration of the ground water, which stimulates aerobic biodegradation of pollutants.

In air sparging, the nature and extent of the air pathways determine the region of influence of remedial process. The efficiency depends on microscopic effects such as the mode of air flow (channels or bubbles) and air channel density as well as macroscopic effects such as the spatial distribution of air paths. Ji et al. [2] show that air travels as stable channels for soil grain sizes of 0.75 mm or less (e.g. fine sands) and as bubbles for soil grain diameters of 4 mm and larger (e.g. medium to coarse gravels). The transition occurs in soil with a grain size of approximately 2 mm, which typically represents medium to coarse sands [3]. The density and distribution of air channels in the subsurface are also affected by operational factors such as air flow rate [4,5], injection pressure [2] and spacing of injection and extraction wells [1,6].

Site geology or subsurface heterogeneity is considered to have significant influence on the efficiency of air sparging remediation. Symmetrical air plume around an injection point is observed in laboratory experiments with homogeneous saturated soil or glass beads [2,7–9], whereas in the field injected air is more likely to travel in channels with

* Corresponding author. Tel.: +44-1223-332713;
fax: +44-1223-339713.
E-mail address: ks@eng.cam.ac.uk (K. Soga).

irregular or asymmetric shape because of the heterogeneous nature of the subsurface [2,10–12]. Reddy and Adams [13] investigated the removal of dissolved phase hydrocarbon under different heterogeneous soil conditions and observed spatial variations in the dissolved phase removal due to soil heterogeneity. They concluded that air would bypass low permeable soils when the permeability ratio between two adjoining layers or lenses is less than 10:1. When bypass occurs, remedial time is governed by the diffusion process of contaminants toward the air channels.

Compared to air sparging remediation of contaminants dissolved in water, remediation of NAPLs in the field is further affected by its complex spatial distribution. Aquifer heterogeneity has been shown to increase the complexity of NAPL movement and subsequent entrapment and the spatial distribution is controlled by unstable fingering, preferential channelling and both micro- (pore) and macro-scale (layering and soil texture contrast) heterogeneity of subsurface formations [14,15]. Final NAPL distribution in these complex geological environments is manifested by zones of entrapment ranging from low saturation (residual, ganglia and blobs) to high saturation (lenses, pools and macro-scale entrapment zones resulting from capillary barriers).

Remediation of NAPL contaminated sites continue to produce significant engineering challenges due to the difficulties in locating the entrapped NAPLs, inability to efficiently remove them from soils, and limitations in the modelling and assessment tools that are designed to predict their fate and transport behaviour. Few studies have been reported to assess the efficiency of air sparging on the removal of NAPLs [6,16,17]. As the distribution of NAPLs in the subsurface is often very complex, it is possible that the design of air sparging system based on homogeneous laboratory test conditions can lead to inadequate performance. There is a need to understand the effect of NAPL entrapment condition on air sparging system efficiency.

Laboratory tank experiments allow evaluation of NAPL removal performance under well-defined heterogeneous soil conditions. The tank provides the facility for placement of layers and lenses with different permeable sands in order to investigate the bypassing and air channel deviations due to local variations in porous media. In this study, experiments were performed to investigate the mass removal of free phase toluene near water table. The soil models had a coarser sand lens inside finer sand matrix and four different NAPL entrapment conditions were created by varying the location of the water table in the models. The performance of air sparging remediation at different entrapment conditions was examined by measuring temporal and spatial toluene concentrations in the models. In some tests, gas and dissolved concentrations were measured after air sparging remediation so that the degree of potential contamination in the post-remediation stage could be assessed.

## 2. Physical modelling of air sparging remediation

2.1. Test setup and materials

A soil tank, which has internal dimensions of 1.2 m (length) × 0.8 m (height) × 0.15 m (width), was used to carry out the experiments. The front surface of the tank is made of toughened glass to achieve the visibility of subsurface during testing. The remaining sides are built with stainless steel. As shown in Fig. 1, there are two wells at the lateral sides of the tank; one is used as an extraction well, whereas the other is opened to the atmosphere. The bottom of the tank is connected to a water tank through a moving reservoir, by which it is possible to control the height of the water table. Two filter papers are placed at the bottom of the tank to prevent the fines from washing out from the tank.

On the backside of the tank, 77 sampling ports of 10 mm diameter are installed as shown in Fig. 2. These ports are used either to obtain gas, water or soil samples before, during, or at the end of the test or to install resistivity probes or tensiometers for continuous measurements of water saturation and liquid pressures during experiment. The sampling ports for collecting gas/liquid samples consist of a rubber septum held in brass fittings.

The air sparging (AS) system consists of a compressor, regulator, pressure gauge, flow meter and sparger as shown in Fig. 1. A plastic silencer (RS Components Ltd., UK) of 38.5 mm diameter and 123.5 mm effective length is used as a sparger to inject air into the soil model. It was fixed at location G6 (see Fig. 2). The soil vapour extraction (SVE) system has a pump, vacuum gauge, regulator and flow meter (see Fig. 1).

Two different unconsolidated sands were used in the experiments. According to the British Standard, they are Fraction B (particle sizes ranging from 0.6 to 1.18 mm and the hydraulic conductivity is 6.13×10^{-3} m/s) and Fraction C (particle sizes ranging from 0.3 to 0.6 mm and the hydraulic conductivity is 9.4×10^{-4} m/s). Both sands were provided by WBB Minerals (UK). Fraction C sand was used as the main body of porous media, while Fraction B sand was used to create a coarser lens in finer Fraction C sand matrix. Fig. 3 shows the location of the coarse sand lens in the sand models.

Toluene, a major constituent of gasoline and other petroleum products, was used as the model LNAPL. Toluene (Fisher Scientific International Company) has high volatility with vapour pressure of 3.79 kPa. It also has fairly high toxicity and the exposure limit of gas is 50 ppm. For the experiments, Toluene was mixed with non-volatile, organic soluble Red Oil O (Aldrich chemical Company Inc.) (0.5 g of dye in 1 l of toluene) to achieve the visibility in the migration through the porous media. The properties of pure toluene are listed in Table 1. Wilkins et al. [18] report that the dye has a negligible effect on contaminant and mass transfer properties.
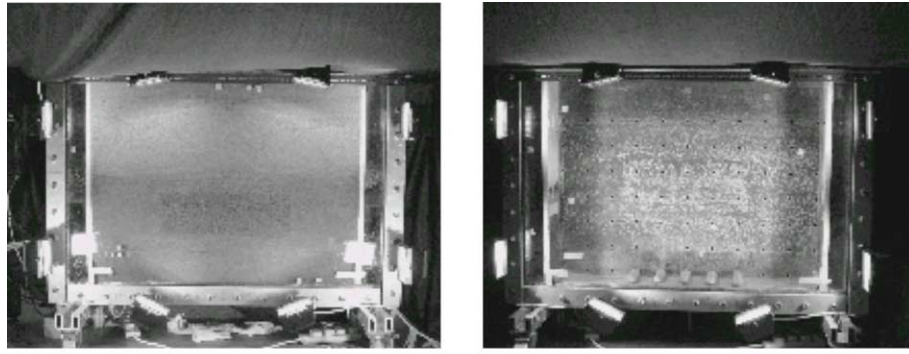
(with sand)   (without sand)

(a) Photos of the tank
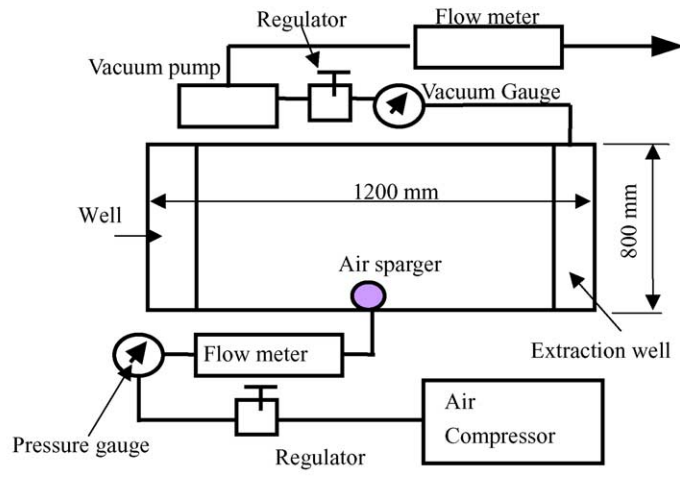
(b) Schematic diagram

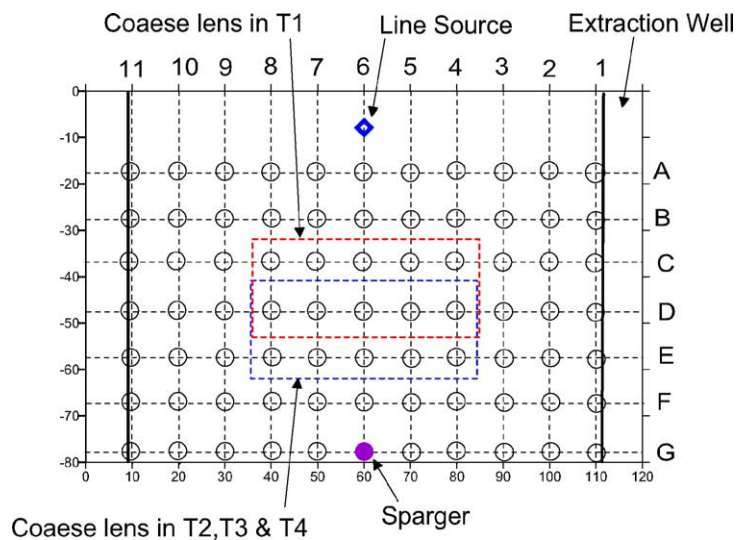Fig. 1. Setup of the two-dimensional air sparging/SVE system.

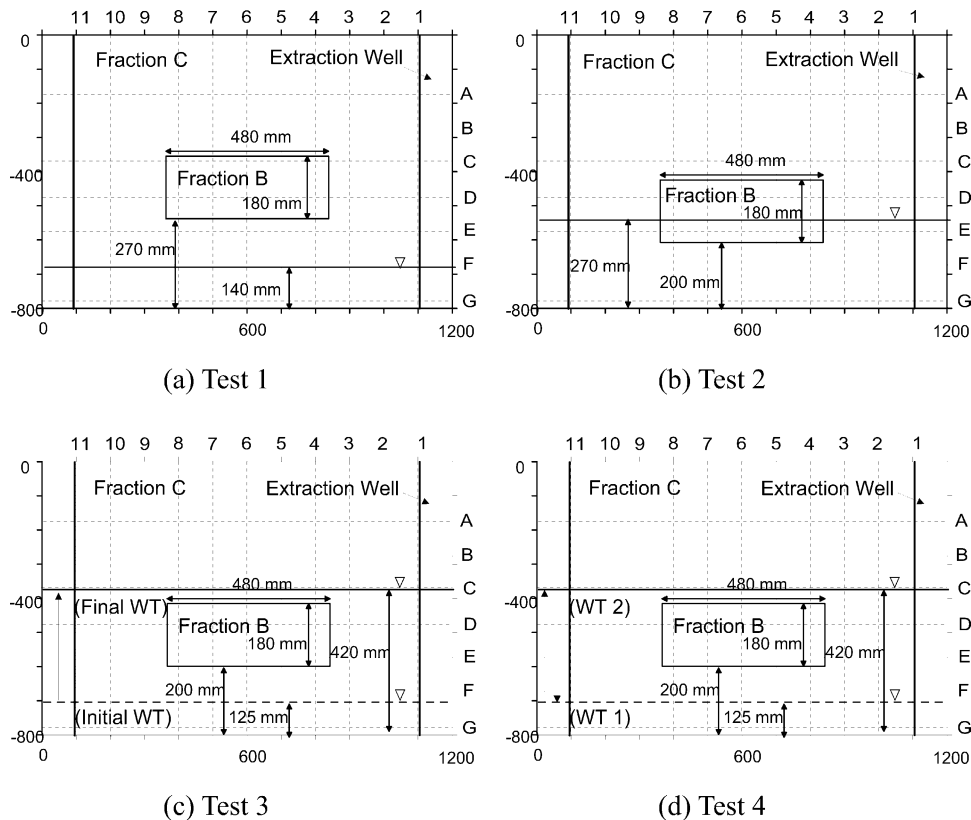Fig. 2. Layout of 77 grid sampling ports.

Fig. 3. Soil models.

2.2. Experimental procedure

Four tank experiments were performed in this study. The water table location was varied to create different LNAPL entrapment conditions and air sparging remediation was performed.

The tank was packed with sands under water (wet packing). During sand packing, the water level in the tank was gradually increased so that it maintained approximately 50 mm above the level of sand surface. The wet packing gave uniform homogeneous sand condition and also provided almost fully saturated condition. In dry packing, air is more likely to trap among the sand particles, which contributes to creating preferential air flows [2]. The average porosity of the fine sand matrix was 0.40.

Two aluminium plates, which are slightly smaller than the width of the tank, were used to create a coarse sand lens in

the middle of fine sand matrix. The plates, with a distance of the length of Fraction B sand lens, were pushed into the Fraction C sand. Fraction B sands were placed in the middle of the two plates to create a coarse sand lens, while Fraction C sands were filled around the coarse sand lens as shown in Fig. 3 without disturbing the stability of the plates. When the height of the coarser sand lens was achieved, the plates were removed. The average porosity of the coarse sand lens was 0.44.

After creating a fully saturated soil model, the water table was lowered gradually to a predetermined level. Before the toluene spill, the water table was placed (i) below the coarse sand lens in Tests 1, 3 and 4 and (ii) in the middle of the coarse sand in Test 2. Resistivity probes and tensiometers were placed at different location of tank to measure the changes in water saturation and pressure during water drainage. The total duration of drainage stage was between 1680 and 3160 min and the readings from resistivity probes and tensiometers confirmed that the model was in hydrostatic condition.

Upon completion of water drainage, toluene was spilled using a line source to create a two-dimensional NAPL plume in the tank. The line source was buried in the middle of the tank, approximately 60–80 mm below from the soil surface (see Fig. 2). Prior to spilling, a rubber membrane was placed over the entire soil surface to ensure that all contaminated vapour would go into the extraction well. The system was

Table 1
Toluene chemical properties

Molecular weight (g/mol)	92.14
Density (g/cm^3 at 20 °C)	0.8669
Vapour pressure (kPa at 5 °C)	3.79
Henry's constant (kPa m^3/mol at 25 °C)	0.66
Solubility (g/l)	0.53
Melting point (°C)	−95
Boiling point (°C)	111
Specific heat (J/g K at 25 °C)	1.71

then sealed by placing a lid on the top of the tank. A total of 8×10^{-4} m^3 (687 g) of toluene was spilled at an average spilling rate of 8000 mm^3/s. Once spilling of toluene was over, the system was left for redistribution until the movement of LNAPL ceased. In Tests 3 and 4, the water table was then raised, so that the toluene trapped in the coarse sand lens is placed below the water table as shown in Fig. 3(c) and (d).

In the AS/SVE stage, air was inject at a flow rate of 0.005 m^3/min from the sparger and extracted at a flow rate of 0.012 m^3/min into the extraction well. Ten cycles of 10 h AS/SVE operational period followed by 14 h of shutdown period were conducted. The AS/SVE stage lasted 10 days. The system interruption was performed to assess the rate-limited behaviour of NAPL–gas mass transfer process [19] and to investigate the spreading of contamination during the shutdown period.

Toluene concentration in the effluent gas was measured to calculate the total mass removed from the system. At selected locations, gas and liquid samples were taken at various time intervals and were analysed to evaluate the spatial and temporal variation of toluene concentration in the tank. Gas and liquid samples were collected using 0.1 and 1 ml gas-tight syringes, respectively. Concentrations of toluene in the gas phase were measured by Agilent 6850 Series gas chromatography with a flame ionisation detector (FID). Aqueous concentration was measured by injecting headspace samples into the gas chromatography. In each case, the sample size of gas was 50 μl. At the end of the experiments, a copper tube with 250 mm length and 9.5 mm diameter was inserted through the sampling ports to collect soil samples, which were then analysed to measure the amount of residual toluene in the tank.

3. Test results and discussion

3.1. LNAPL entrapment

By changing the location of the water table in the tank, four different entrapment conditions were achieved, simulating possible conditions encountered in the field near the water table. Fig. 4 shows the final entrapments of toluene in all four experiments. In Test 1, the water table was placed at the bottom of the tank, as shown in Fig. 3(a). During the spilling stage, the majority of toluene migrated through the coarse sand lens and finally rested in the fine sand capillary zone with some lateral spreading, as shown in Fig. 4(a). In Test 2, the water table was placed at the mid-height of the coarse sand lens. Most of the spilled toluene was trapped at high NAPL saturation in the top region of the coarse sand lens, as shown in Fig. 4(b), because the lower part of the lens was saturated with water.

In Test 3, the water table was placed below the lens during the spill stage, as shown in Fig. 3(c) and the toluene pooled on the bottom interface of two sands initially, as shown in

Fig. 4(c-1). After the spill, the water table was raised above the lens as shown in Fig. 3(c) and the toluene spread through out the coarse sand lens by the buoyancy force. As shown in Fig. 4(c-2), the majority of the toluene was entrapped in the lens due to capillary barrier effect at the top layer interface.

In Test 4, the same condition of Test 3 was created initially, as shown in Fig. 4(d-1), but then the water table was lowered (to WT 1) before the air sparging operation, as shown in Fig. 3(d). As a result, uniformly distributed toluene inside the coarse sand lens came down and entrapped on the bottom layer interface, as shown in Fig. 4(d-2). Test 4 was performed to examine the effect of artificial control of water table on air sparging remedial efficiency.

3.2. LNAPL removal

In Tests 1–3, AS/SVE was performed by ten cycles of 10 h of operating period followed by 14 h of shutdown period and the water table was kept constant throughout the operation. In Test 4, the same numbers of cycle were performed, but the water table was lowered 18 h before the operation and then raised in steps every 48 h until it came back to the original water table, which was above the coarse sand lens.

As air was injected from the bottom centre of the tank, it travelled through the porous media in the form of pore-scale air channels in all four tests. The zone of influence in the fine sand matrix increased gradually with height until it reached to the coarse sand lens. Once injected air entered into more permeable lens, air channels passed vertically through the medium.

The gas concentration of toluene at the extraction well declined with time in all four tests, indicating gradual mass removal from NAPL to the gas phase. Fig. 5 shows the change in gas concentration with operational time measured in Test 2. The spikes shown are the increased gas concentrations immediately after the shutdown period. At the beginning of the extraction, the measured gas concentrations were close to the vapour pressure of toluene achieving the local equilibrium condition. As the gas concentration at the extraction well gradually decreased with the extraction time, the spikes become more apparent because additional toluene gas was generated from the source during the shutdown periods. The toluene gas concentration at the extraction well at the end of the 10 cycles of AS/SVE operation was between 0.15 and 0.5 mg/l in all four experiments. Visual observation of the tank after the remediation also indicated that most of the red areas of dyed toluene had disappeared.

The reducing gas concentration in Fig. 5 can be attributed to (i) incomplete NAPL–air contact by preferential air flow paths affected by soil heterogeneity and non-uniform NAPL distribution, (ii) the rate-limited mass transfer behaviour from NAPL to the gas phase, and (iii) the rate-limited mass transfer from the dissolved aqueous phase to the gas phase. The latter two can also contribute to the increased gas concentration observed after shutdown period. It is also

(a) Test 1

(b) Test 2

(c-1) Test 3
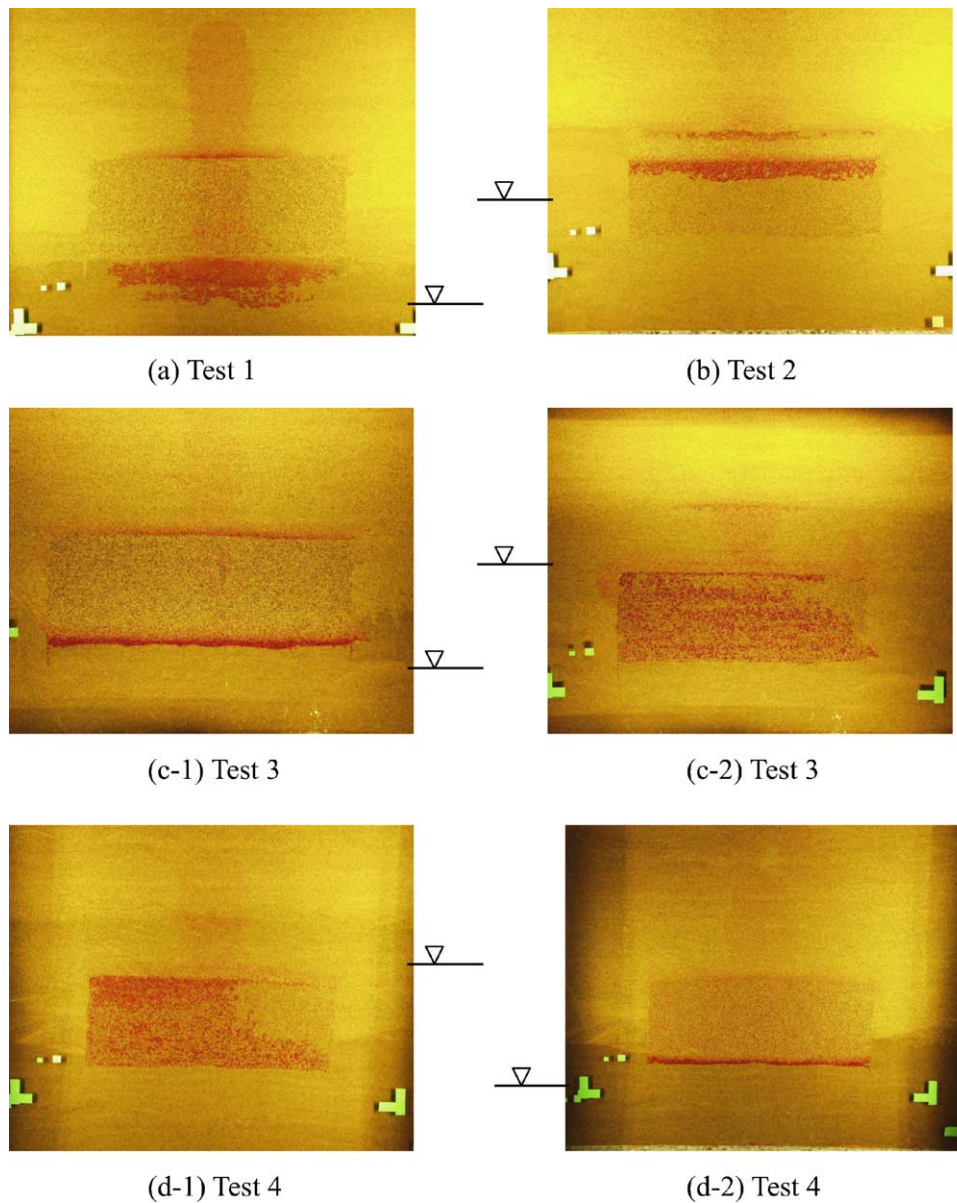
(c-2) Test 3

(d-1) Test 4

(d-2) Test 4

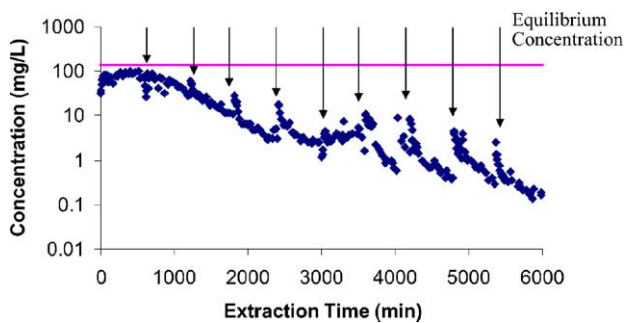Fig. 4. Final distribution of toluene.

Fig. 5. Variation of toluene gas concentration at extraction well with extraction time in Test 2 (arrows show the start of extraction cycle).

possible that the remaining NAPL mobilised and redistributed during the shutdown periods as a result of water flowing back into air flow paths. Ji et al. [2] and Ahlfeld et al. [12] suggest from their experimental observation that small variation of micro-scale heterogeneities was enough to change the air flow pattern in the porous media. Since the interfacial tension of air–toluene is smaller than that of air–water, air can preferentially flow towards toluene. This brings the better contact of air with entrapped NAPL, which was not in the vicinity of air channels in previous cycle. Therefore, when AS/SVE was resumed, a new air channel system was formed due to new micro-scale NAPL entrapment condition. Moreover, mixing of toluene with contaminant free water improves the dissolution due to the availability of higher concentration gradient than that in
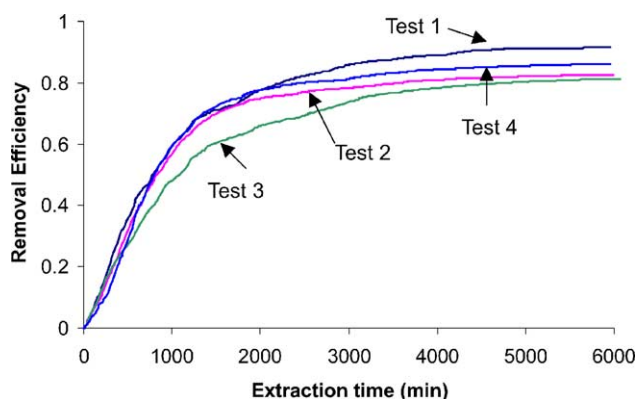
Fig. 6. Mass removal efficiency.

partially contaminated water. This may also contributed to the increase in gas concentration after the shutdown periods.

The mass removal from the tank can be computed from the measured gas concentration–time curves for a given extraction flow rate. The computed mass removal efficiencies with time are shown in Fig. 6 for all four tests. The mass removal efficiency is defined as the amount of NAPL mass removed compared to the initially spilled mass. The mass removal rates of four tests were very similar at the beginning. The toluene was well in contact with air channels due to high saturation of toluene resulting high mass removal. However, with time, the mass removal rate decreased mainly due to loss of contact of toluene with air channels. As free phase toluene was removed, the direct contact between NAPL and air reduced at the later stage of the remediation. For NAPLs not in contact with air, it has to dissolve into the aqueous phase first and then to vaporise into the gas phase. This leads to slow mass partitioning process driven by diffusion process of toluene in the aqueous phase, contributing to long tail mass removal.

The mass removal efficiency at the end of the experiment was approximately 91% in Test 1, in which the majority of the NAPL was not trapped in the coarse sand lens. On the other hand, lower efficiencies of 82 and 81% were obtained in Test 2 and Test 3, respectively, in which larger portion of the spilled NAPL was entrapped in the coarse lens. In Test 4, the mass removal efficiency increased to 86% where the water table was brought up step by step during the AS/SVE.

In Test 1, toluene trapped below the coarse sand lens near the injection source. The entrapped toluene was in the high-density air plume increasing the NAPL–air interfacial mass transfer area. The NAPL entrapped in the unsaturated zone also volatilised quickly by the soil vapour extraction. Compared to Test 1, the other three tests, in which NAPL was trapped in the sand lens, showed lower final removal efficiencies. Tests 2 and 3 had limited contribution from the soil vapour extraction; Test 2 had a thin water layer above the coarse lens due to high capillary zone of the fine sand matrix, whereas the water table in Test 3 was above the sand lens.

In Test 3, although it showed a similar initial mass removal rate, it has deviated considerably from the other curves after 600 min as shown in Fig. 6. In this experiment, toluene was uniformly distributed in the coarse lens. It is possible that this uniform distribution of toluene hence the low average NAPL saturation reduced the contact surface area between NAPL and air, resulting in a low mass removal rate. In contrast, the other two tests (Tests 2 and 4) with NAPL entrapped in the coarse sand lens had a more localised zone of high NAPL saturation as shown in Fig. 4.

Tests 3 and 4 had the same NAPL entrapment condition after raising the water table, but the water table in Test 4 was lowered just before the AS/SVE and it was raised back to the original condition during the AS/SVE. The raising of water table step by step during AS/SVE resulted in a better final removal efficiency of 86% in Test 4 compared to 81% in Test 3. A zone of high NAPL saturation was achieved by lowering the water table as shown in Fig. 4(d-2) and this increased the NAPL–air contact surface area as well as the increased contribution of SVE system. Furthermore, variation of water table enhanced mixing of toluene with contaminant free water and hence improved the dissolution. These results show that, when toluene is entrapped in a coarser sand lens, higher cumulative mass removal was achieved by remobilising and redistributing the free phase toluene.

3.3. Mass transfer during shutdown period and after remediation

The experimental results show that complete removal was not possible and the degree of removal was affected by initial NAPL entrapment condition as well as the change in entrapment condition during AS/SVE. Accepting this limitation, the following question arises; what is the potential likelihood of contamination spreading after incomplete removal of the NAPL source? There is a need to understand the mass transfer process through the volatilisation or dissolution after remediation, so that any risk of further contamination in the post-remediation stage is in an acceptable level.

Understanding the mass transfer process during shutdown period allows examination of further increase in potential gas contamination by incomplete NAPL removal by AS/SVE. The rebound in gas concentration at the extraction well before and after the shutdown period is plotted against the amount of toluene left inside the soil models, as shown in Fig. 7. It was found that the amount of concentration rebound after 14 h of shutdown period was linearly reduced with the amount of toluene left in the system. For a given toluene volume, Test 3 gave the smallest rebound since most of the NAPL was entrapped below the water table, whereas Test 1 had the largest rebound because majority of the NAPL was left in the unsaturated zone. Test 4 had a large rebound at the beginning when large volume of unsaturated zone was created during the lowering of the water table. However, the amount of rebound decreased as the water table was raised. Extrapolation of the trend lines shows that the rebound will
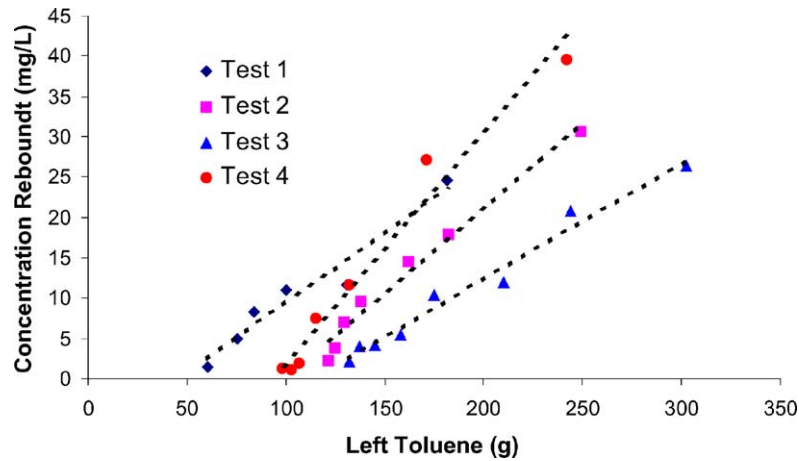
Fig. 7. Variation of concentration increment with the amount of toluene left in the soil.

be negligible when NAPL is left about 100 g in the sand lens. On the other hand, in Test 1, a much larger removal of NAPL was necessary to achieve the same condition.

The potential gas/water contamination after AS/SVE remediation was examined in Tests 2 and 4, in which gas/liquid samples at various locations of the tank were collected for 10 days after AS/SVE operation. Fig. 8 shows the spatial distribution of gas phase concentrations at different times for Test 2. Immediately after remediation, the gas concentrations were between 0.5 and 1 mg/l as shown in Fig. 8(a). However, as shown in Fig. 8(b) and (c), the gas concentrations within the soil model increased gradually and spread from the source zone area giving the maximum concentration of 6 mg/l after 10 days.

Fig. 9 shows the spatial distribution of aqueous phase toluene concentrations at different times after remediation in Test 2. The initial spatial distribution of dissolved toluene in Test 2 just after the remediation was very narrow and the maximum concentration was measured near the right end of the air–water interface as shown in Fig. 9(a). As more toluene dissolved from the remaining NAPL source with

time, the area of high concentration increased; the maximum concentration of 86 mg/l was measured in the middle of the soil model 233 h after the remediation as shown in Fig. 9(c). The gas/water concentration measurements indicate that the majority of the remained NAPL source exists in the middle of the tank, where it was more likely to have direct contact between air and NAPL after remediation. Soil samples taken after the test confirm this by providing high soil concentration of 48 mg/kg at the middle of the tank.

Figs. 10 and 11 show the changes in spatial distribution of gas and water concentrations after remediation for Test 4. The measured gas concentrations in Fig. 10 are much smaller than those in Test 2 (Fig. 8), whereas the aqueous phase concentrations in Fig. 11 are larger than those in Test 2 (Fig. 9). More toluene was trapped in the saturated zone in Test 4, whereas more toluene was trapped inside the coarse sand lens above the water table in Test 2. In Fig. 11, two largely concentrated zones are located away from the middle area, suggesting that the remained free phase toluene was located in these two zones. Corresponding to this, the gas concentrations are higher at two sides of the tank compared
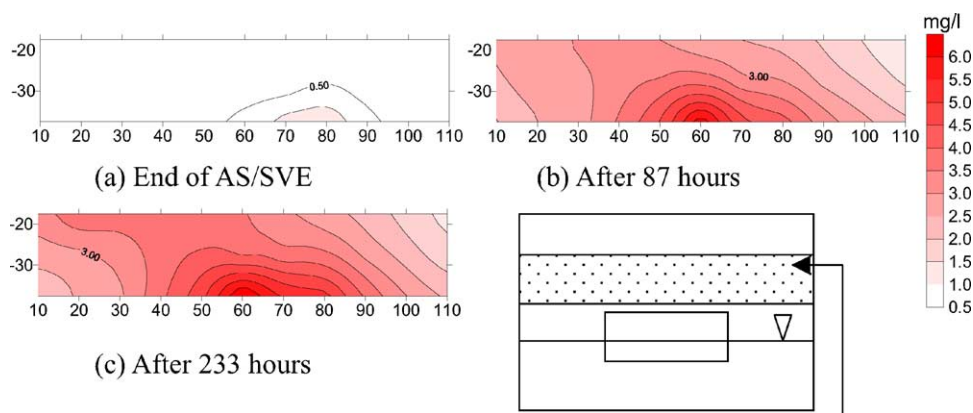
Fig. 8. Spatial distribution of toluene gas concentration at different times for Test 2.
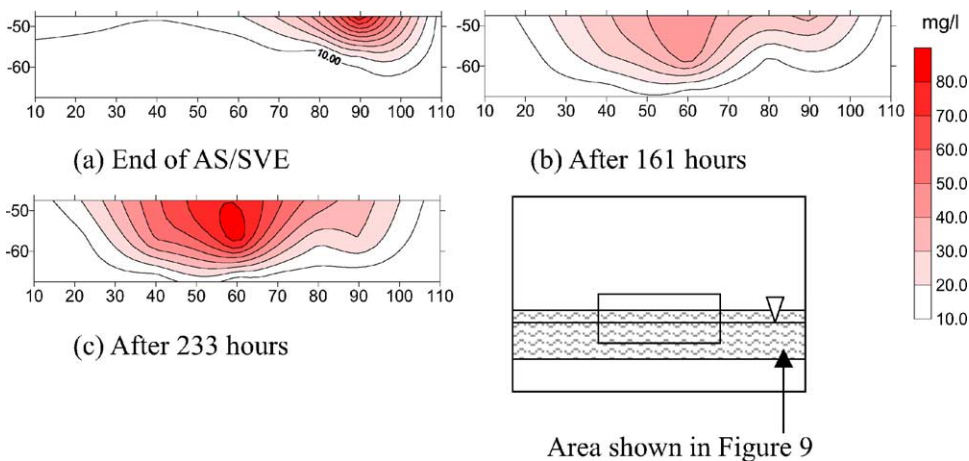
Fig. 9. Spatial distribution of dissolved toluene concentration at different times for Test 2.
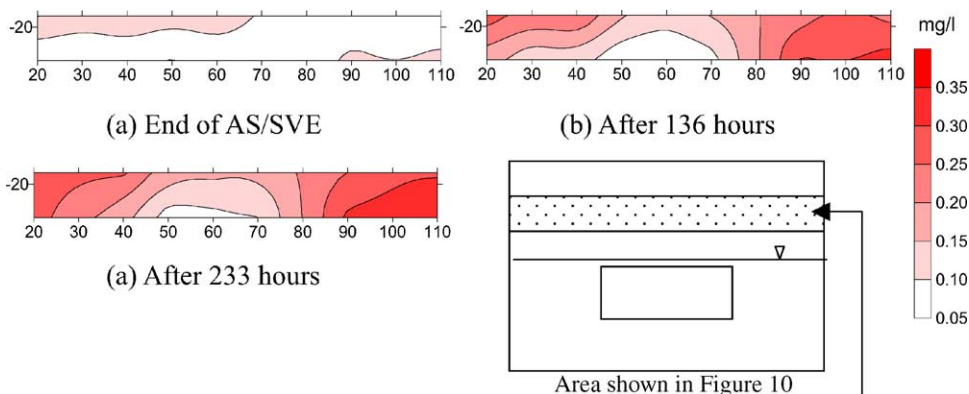

Fig. 10. Spatial distribution of toluene gas concentration at different times for Test 4.

to the middle as shown in Fig. 10. Measured soil sample after the test also showed relatively high soil concentrations at the two sides of the tank.

Fig. 12 shows the changes in gas concentration with time at selected sample ports in Tests 2 and 4. The gas concentration at the locations near the remained NAPL (C6 and B6 in Test 2, B11 and B2 in Test 4) increased rapidly at the beginning but reached to steady state values. Smaller steady state values were obtained at locations far away from the source (e.g. A11 in Test 2).

Fig. 13 shows the aqueous phase concentration at selected locations. In contrast to gas sample data shown in Fig. 12, a linear increase in aqueous phase concentration with time is observed at locations where free phase toluene
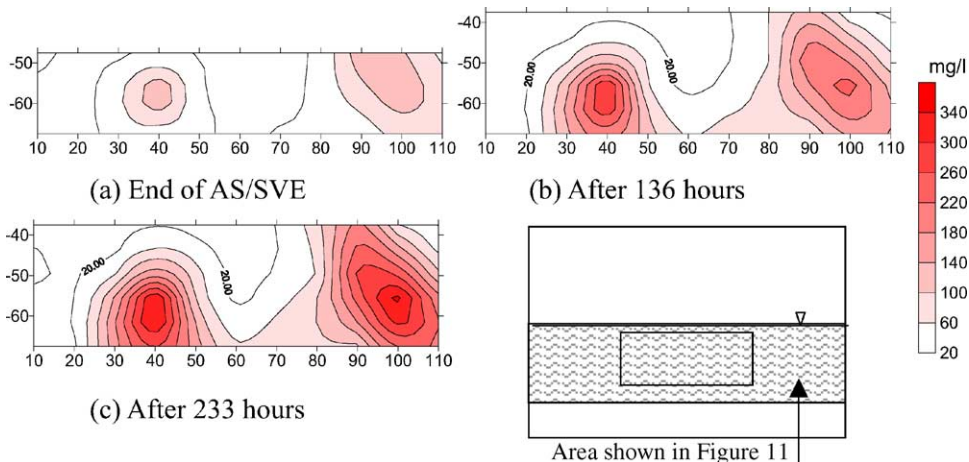

Fig. 11. Spatial distribution of dissolved toluene concentration at different times for Test 4.
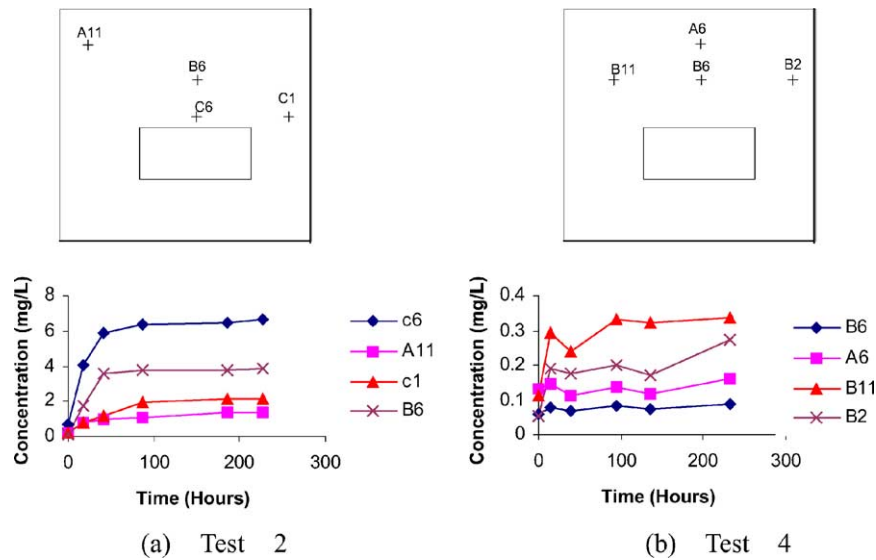
Fig. 12. Variation of gas toluene concentration at some sample ports after remediation (see Fig. 2 for the exact location of sampling ports).
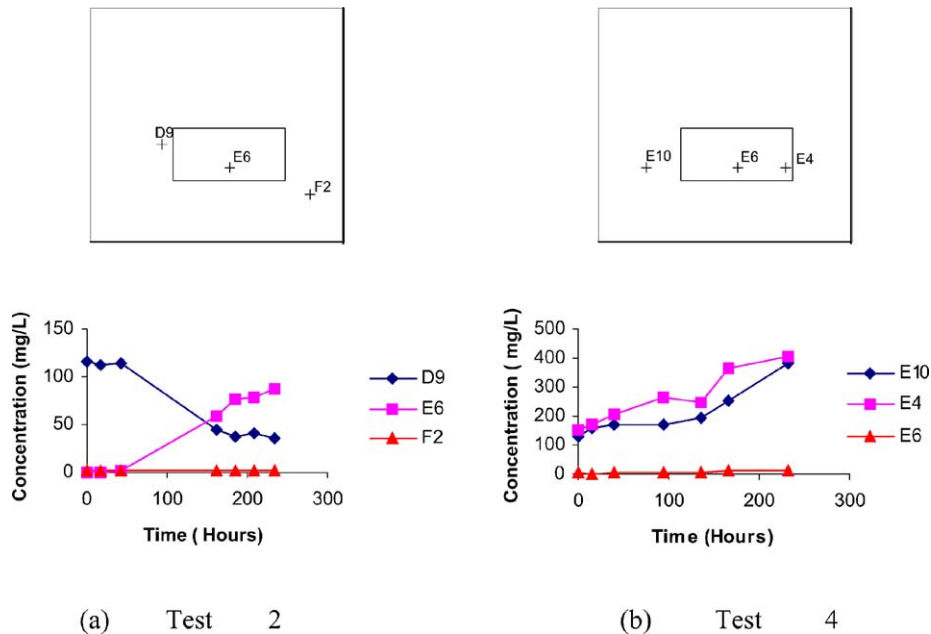

Fig. 13. Variation of dissolved toluene concentration at some sample ports after remediation (see Fig. 2 for the exact location of sampling ports).

was left. Compared to Test 2, the increase in Test 4 is much larger reaching toward the solubility limit of 530 mg/l because more toluene is left below the water table. For locations away from possible free phase toluene (e.g. A11 and C1 in Test 2, B6 and A6 in Test 4), there is a very small increase with time. The aqueous phase concentration at D9 in Test 2 decreased with time, indicating possible diffusion or volatilisation from this initially concentrated area as shown in Fig. 9. The continuous increase in the aqueous phase concentrations with time is different from the gas concentrations, which reached some steady state values. The results indicate that the time-dependent mass transfer process of the aqueous phase is different from that of the gas phase, which

requires further investigation to quantify potential risk of contamination after remediation with incomplete free phase removal.

4. Conclusions

The effect of soil heterogeneity and the entrapment condition of LNAPL source zone on the mass removal efficiency of AS/SVE was investigated using a two-dimensional laboratory soil tank. It was observed that different mass removal efficiencies were achieved for different NAPL entrapment conditions, which was controlled by soil heterogeneity and

location of water table before and during AS/SVE operation. The best efficiency of 91% was obtained when the majority of the spilled NAPL was placed in the fine sand matrix, where lower efficiencies were obtained when the NAPL was trapped in coarse sand lens. Within the latter cases, a better efficiency was achieved when LNAPL was trapped in the lens with high saturations. A randomly distributed NAPL source with a low saturation gave the lowest removal efficiency due to small NAPL–air contact surface area. Remobilization and redistribution of toluene and water and the resulting microstructure alteration in the system also improved the mass removal.

In general, the overall result highlighted the fact that it is very difficult to remove NAPL source completely due to complex entrapment of NAPL in heterogeneous soil system. The data obtained during the shutdown periods and after AS/SVE were used to assess any risk of potential contamination by the remaining NAPL source. It was found that, for a given entrapment condition, the rebound concentration at the extraction well immediately after the shutdown period was linearly with the amount of toluene left in the soil model. After AS/SVE remediation, the gas concentration near the remaining source zone in the tank increased rapidly to steady state values that are much less than the vapour pressure, whereas the aqueous phase concentration continuously increased with time. These results provide preliminary insight of how toluene mass comes out from an incompletely removed NAPL source into the gas and aqueous phases after remediation.

References

[1] US EPA, Analysis of selected enhancements for soil vapor extraction, EPA-542-R-94-009 (1997).

[2] W. Ji, A. Ahlfeld, D.P. Lin, E. Hill, Laboratory study of air sparging: air flow visualization, Groundwater Monitor. Remediat. 13 (4) (1993) 115–127.

[3] R. Semer, J.A. Adams, K.R. Reddy, An experimental investigation of air flow patterns in saturated soils during air sparging, Geotech. Geolog. Eng. 16 (1998) 59–75.

[4] A. Leeson, R. Hinchee, G. Headington, C. Vogel, Air channel distribution during air sparging: a field experiment, in: R. Hinchee, R. Miller, P. Johnson (Eds.), In Situ Aeration: Air Sparging, Bioventing and Related Remediation Processes, Battelle, Columbus, Ohio, 1995, pp. 215–223.

[5] K. Rutherford, P. Johnson, Effects of process control changes on aquifer oxygenation rates during in situ air sparging in homogeneous aquifers, Groundwater Monitor. Remediat. 16 (4) (1996) 132–141.

[6] S.W. Rogers, S.K. Ong, Influence of porous media, airflow rate and air channel spacing on benzene NAPL removal during air sparging, Environ. Sci. Technol. 34 (2000) 764–770.

[7] C. Elder, C. Benson, Air channel formation, size, spacing and tortuosity during air sparging, Groundwater Monitor. Remediat. 19 (1999) 171–181.

[8] J.W. Peterson, M.J. DeBoer, K.L. Lake, A laboratory simulation of toluene cleanup by air sparging of water-saturated sands, J. Hazard. Mater. 72 (2000) 167–178.

[9] J.A. Adams, K.R. Reddy, Removal of dissolved- and free-phase benzene pools from ground water using in situ air sparging, J. Environ. Eng. 126 (8) (2000) 697–707.

[10] R. Johnson, P. Johnson, D. McWorter, R. Hinchee, I. Goodman, An overview of in situ air sparging, Groundwater Monitor. Remediat. 13 (4) (1993) 127–134.

[11] R.E. Hinchee, Air sparging state of the art, in: R.E. Hinchee (Ed.), Air Sparging for Site Remediation, Lewis, 1994, pp. 1–12.

[12] D. Ahlfeld, A. Dahmani, W. Ji, A conceptual model of field behavior of air sparging and its implications for application, Groundwater Monitor. Remediat. 14 (1994) 132–139.

[13] K.R. Reddy, J.A. Adams, Effect of soil heterogeneity on airflow patterns and hydrocarbon removal during in situ air sparging, J. Geotech. Geoenviron. Eng. 127 (3) (2001) 234–247.

[14] F. Schwille, Dense Chlorinated Solvents in Porous and Fractured Media-model Experiments, English Language Ed., Lewis Publishers, 1988.

[15] T.H. Illangasekare, E.J. Armbruster III, D.N. Yates, Non-aqueous-phase fluids in heterogeneous aquifers—experimental study, J. Environ. Eng. 121 (8) (1995) 571–579.

[16] P.C. Johnson, A. Das, C. Bruce, Effect of flow rate changes and pulsing on the treatment of source zones by in situ air sparging, Environ. Sci. Technol. 33 (10) (1999) 1726–1731.

[17] W.A.P. Waduge, K. Soga, J. Kawabata, Laboratory testing of air sparging/SVE system for remediation of NAPLs entrapped in heterogeneous soil, in: Proceedings of the International Conference on Physical Modelling in Geotechnics, ICPMG'02, 2002, pp. 373–378.

[18] M.D. Wilkins, L.M. Abriola, K.D. Pennell, An experimental investigation of rate-limited nonaqueous phase liquid volatilization in unsaturated porous media: steady state mass transfer, Water Resour. Res. 31 (9) (1995) 2159–2172.

[19] M.L. Brusseau, Q. Hu, R. Srivastava, Using flow interruption to identify factors causing nonideal contaminant transport, J. Contam. Hydrol. 24 (1997) 205–219.